Journal of Visualization, Vol. 11, No. 4 (2008)285-298

Regular Paper

Turbulent Passive Scalar Transport under Localized Blowing

Tardu, S.* and Doche, O.*

* Laboratoire des Ecoulements Géophysiques et Industriels (LEGI), B.P. 53 X 38041 Grenoble, Cédex France. E-mail: Sedat. Tardu@hmg.inpg.fr

Received 6 October 2007
Revised 22 May 2008

Abstract : The effect of blowing through a localized slot on the wall turbulence dynamics and heat transfer process is analyzed by direct numerical simulations in a fully developed turbulent channel flow. The severity parameter is mild and there is no flow separation induced by the blowing. The shear stress transport and temperature energy budget is discussed in detail. The wall shear and flux decreases immediately downstream the slot in a similar manner but the Reynolds analogy does not hold over the slot. The physical process is governed by the production and pressure redistribution over the slot in a complex manner. The turbulent transport and especially the advection play an essential role in the heat transfer mechanism.

Keywords : Localized blowing, Control of Wall turbulence, Direct Numerical Simulations, Heat transfer.

1. Introduction

The control of the turbulent drag and the heat transfer is of great industrial importance, and has serious consequences on environment. A huge effort is paid since a decade to find active methods and strategies to decrease the drag, since passive devices have only limited efficiency. It is theoretically possible to laminarize a turbulent wall flow by optimal control. Yet, the latter is totally unfeasible from a technical point of view because it requires an unacceptably dense distribution of the MEMS (Micro Electro Mechanical Systems) sensors and actuators at the wall. Large-scale control methodologies, easy to realize are therefore still needed, at least from a practical point of view. The best feasible way to structurally modify the wall turbulence is to intervene directly at the wall. Localized constant blowing through strips is part of these strategies.

It is well known that, generally speaking, low and moderate suction increases the wall shear stress, but decreases the turbulence in the inner layer. The role of blowing is opposite. There has been an increasing interest in studying the effect of local (steady) suction through spanwise slots in recent years (Sokolov and Antonia, 1993; Sano and Hirayama, 1985). These studies are quite detailed, including the effect on the fine structure of the near wall turbulence, the distribution in the quadrants, the bursting activity etc. Quite surprisingly, and although uniformly distributed (porous surface) blowing is well known since longtime, the effect of steady localized blowing through slots has not attracted as much attention, until relatively recently (Tardu, 1998; Park and Choi, 1999). Most of these works are experimental except Park and Choi (1999) who used direct numerical simulations to analyze the effect of localized both suction and blowing. In the latter case however, the blowing is so severe that the flow separates downstream the slot. That constitutes somewhat a disadvantage in practical situations and the physics of the near wall flow is rendered more complex under the

combined effects of the local blowing and separation. The motivation of the present investigation lies on these reasons, and the main aim is to analyze the effect of the local blowing on the wall turbulence and the heat transfer with only a mild severity parameter to avoid the separation.

The paper is divided into four parts. The details of the Direct Numerical Simulations used in this investigation are given in the next session. We expose the flow configuration, the details concerning the localized blowing together with validation of the numerical procedure is given in a separate part. We also discuss detailed flow visualizations of the coherent near wall structures and the associated instantaneous field in this session. This is followed by the presentation of the results related to the effect of the localized blowing, in particular those concerning the transport equations of the Reynolds shear stresses and temperature fluctuations.

2. Direct Numerical Simulations

The direct numerical simulations (DNS) code used here is of finite difference type combined with fractional time procedure. The non-linear terms are explicitly resolved by an Adams-Bash forth scheme. Periodical boundary conditions are used in the homogeneous streamwise and spanwise directions. The size of the computational domain is $(4\pi h \times 2h \times 1.33\pi h)$ in respectively the streamwise x, wall normal y and spanwise z directions, h standing for the channel half width. In terms of wall units $\ell_\nu = \frac{\nu}{u_\tau}$ where ν and u_τ are the viscosity and the shear velocity, the non-dimensional box size is $(2260 \times 360 \times 752)$. Thus the streamwise computational extend is twice larger than the maximum correlation length, while it is roughly eight times larger than the mean streak spacing in the spanwise direction. There are $(513 \times 129 \times 129)$ computational modes in (x, y, z). Uniform and stretched coordinates are used in the streamwise, spanwise and wall normal directions. The first mesh from the wall is at 0.2 wall units. The mesh sizes in the x and z directions are respectively 4.5 and 5.5 ℓ_ν. The Reynolds number based on the channel height and the centerline velocity is fixed at $Re = \frac{hU_c}{\nu} = 4200$ corresponding to $Re_\tau = \frac{hu_\tau}{\nu} = 180$. The computational time step is $\Delta t^+ = \frac{\Delta t}{\ell_\nu} u_\tau = 0.1$.

The simulation of passive scalar transport, is performed through the resolution of the equation $\frac{\partial T}{\partial t} + \frac{\partial (u_j T)}{\partial x_j} = \frac{1}{RePr} \frac{\partial^2 T}{\partial x_j^2}$ where Pr is the Prandtl number. The resolution of this equation requires the calculation of the velocity field at the same time. So, the Direct Numerical and Heat transfer simulations have to be performed simultaneously. The numerical complexity is quite similar to the DNS resolution and similar tools can be employed. A, Runge Kutta (3^{rd} order) scheme is applied for the time advancement while the diffusive term is resolved by a direct LU decomposition. The numerical cost of the heat transfer resolution is quite low and corresponds approximately to 1/5 of the DNS one.

3. Flow Configuration, Data Analysis and Validation

The flow is locally forced through steady blowing by a slot as shown in Fig. 1. The sizes of the slot in wall units in the streamwise l_x^+ and spanwise l_z^+ directions are shown on this figure. Hereafter $(\,)^+$ refers to quantities scaled by the inner variables namely the viscosity ν and the shear velocity $u_\tau = \sqrt{\frac{\tau}{\rho}}$ where τ is the wall shear stress and ρ is the density. The $(\,)^+$ designates also the

temperature don dimensionalized by the wall temperature T_τ i.e., $T^+ = \frac{T}{T_\tau}$ with $T_\tau = \frac{(\partial T/\partial y)_{y=0}}{Re_\tau Pr}$. The channel is submitted to constant temperatures T_{inf} and T_{sup} at the lower and upper walls. The modified temperature is defined as $\theta = \left| \frac{T(x,y,z,t) - T_{inf}}{T_{inf} - T_{sup}} \right|$.

In flows with uniformly distributed continuous blowing/suction (transpired layers through porous surface), the parameter that characterizes the intervention at the wall is given by $B_f = v_0^+ U_\infty^+$ where v_0 stands for the injection/suction velocity at the wall and U_∞ is the boundary layer free stream velocity (which is the centerline velocity in the case of internal flow, Andersen et al., 1975). This is expected, since B_f appears directly in the momentum integral equation of the transpired boundary layer and plays a role similar to the Clauser pressure-gradient parameter. However, the characterization of the severity of local blowing/suction by strips is not straightforward and B_f is not suitable for describing the flow characteristics past the local intervention, as clearly shown by Sano and Hirayama (1985) and Sokolov and Antonia (1993). Indeed, the local suction/blowing involves phenomena related to the relaxation of near wall turbulence downstream of the intervention zone. When v_0^+ is low, but the injection is done over large areas as in transpired boundary layers, the flow has enough time to relax and reach its equilibrium state rapidly. On the other hand, in case of large injection velocities v_0^+ over short distances by strips, the near wall turbulence can hardly maintain its equilibrium state and its structure is expected to be strongly affected (Sokolov and Antonia, 1993). Therefore, $B_f \propto v_0^+$ cannot be a similarity parameter in such cases. The ratio of the injection or suction flow to the *incoming* flow rate, $\beta = \frac{v_0 l_x}{\int_0^h \bar{u}\, dy}$ is therefore introduced by the authors cited before, and proved to be adequate to measure the blowing/suction severity. The severity parameter used here is very small $\beta = 0.006$ and there is strictly no flow separation downstream the slot.

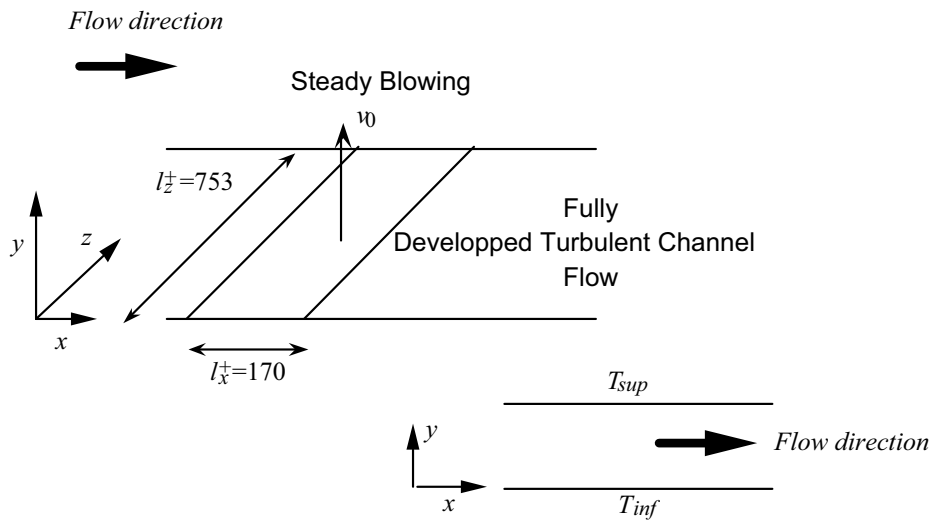

Fig. 1. Flow configuration.

The data is analyzed in detail, in particular, through the transport equations. The Reynolds shear stress transport equation is of the classical form:

$$\frac{\partial}{\partial t}\left\langle u_i' u_j' \right\rangle = A_{ij} + P_{ij} + T_{ij} + D_{ij} + N_{ij} - \varepsilon_{ij} \tag{1}$$

where mixed notations are used for convenience, with u_i' corresponding respectively to the fluctuating streamwise u', wall normal v' and spanwise w' velocity components for $i = 1,2,3$. The bracket $\langle\ \rangle$ stands for averaged quantities. The terms appearing on the right hand side of the Eq. 1 are respectively the advection term $A_{ij} = -\left\langle u_i' u_j' \right\rangle_{,k} \left\langle u_k \right\rangle$ with $(\ )_{,k} = \frac{\partial}{\partial x_k}$ ($x_k = x, y, z$ for $k = 1,2,3$), the production term $P_{ij} = -\left[\left\langle u_i' u_j' \right\rangle \left\langle u_{j,k} \right\rangle + \left\langle u_j' u_k' \right\rangle \left\langle u_{i,k} \right\rangle\right]$, the turbulent transport term $T_{ij} = -\left\langle u_i' u_j' u_k' \right\rangle_{,k}$, the diffusion $D_{ij} = \left\langle u_i' u_j' \right\rangle_{,kk}$, the pressure-velocity correlation term $N_{ij} = -\left[\left\langle u_i' p_{,j}' \right\rangle + \left\langle u_j' p_{,i}' \right\rangle\right]$, and the dissipation $\varepsilon_{ij} = 2\left\langle u_{i,k}' u_{j,k}' \right\rangle$. Figure 2(a) shows the distribution of the corresponding terms in the Reynolds shear stress $-\left\langle u'v' \right\rangle$ ($i = 1, j = 2$) in the standard fully developed turbulent channel flow. These results are in excellent agreement with Mansour et al. (1988). Figure 2(b) shows the contribution of different terms appearing in the temperature fluctuations transport equations that read for

$$\frac{1}{2}\frac{\partial}{\partial t}\left\langle T'^2 \right\rangle = A + B + C + D + E \tag{2}$$

where $A = -\frac{1}{2}\left\langle u_k \right\rangle \left\langle T'^2 \right\rangle_{,k}$ is the advection, $B = -\frac{1}{2}\left\langle u_k' T'^2 \right\rangle_{,k}$ represents the turbulent transport, $C = -\left\langle u_k' T' \right\rangle_{,k} \left\langle T' \right\rangle_{,k}$ is the production, $D = \frac{1}{2PrRe}\left\langle T'^2 \right\rangle_{,kk}$ is the viscous diffusion and $E = -\frac{1}{PrRe}\left\langle T_{,k}' T_{,k}' \right\rangle$ is the dissipation in non-dimensional forms. Figure 2(b) shows the distributions of these terms in the standard turbulent channel flow. There is excellent agreement between these results and Lyons et al. (1991) and Kawamura et al. (1998).

The role played by the near wall coherent structures in the passive scalar transport phenomena is crucial. The quasi-streamwise vortical structures that are generic of the wall turbulence are detected by the λ_2 technique described in Jeong and Husain (1995) and recently discussed in Chakraborty et al. (2007). It is recalled that the λ_2 technique is based on the second negative eigenvalue of the $\mathbf{S^2} + \mathbf{\Omega^2}$ where $S_{ij} = \frac{1}{2}\left(u_{i,j} + u_{j,i}\right)$ is the symmetric and $\Omega_{ij} = \frac{1}{2}\left(u_{i,j} - u_{j,i}\right)$ is the antisymmetric component. Figure 3(a) shows a snapshot of the quasi-streamwise vortices (QSV) and the instantaneous temperature distribution in wall units. It is clearly seen that there is a huge mixing effect of the coherent structures and that the mixing is clearly associated with the presence of the vortices. This is more clearly seen in video that can be provided on demand. The QSV induce strong sweeps (quadrant 4) and ejection (quadrant 2) events that are strongly correlated leading to the generation of high Reynolds shear stress intermittently. Although the QSV are located in majority in the buffer layer at $y^+ = 20$ their purely cinematic effect on the mixing extends to low log-layer even going till the centerline quite often. The difficulty of actively controlling the wall turbulence to break-up the Reynolds analogy to achieve both drag reduction and wall transfer increase is undoubtedly a difficult task.

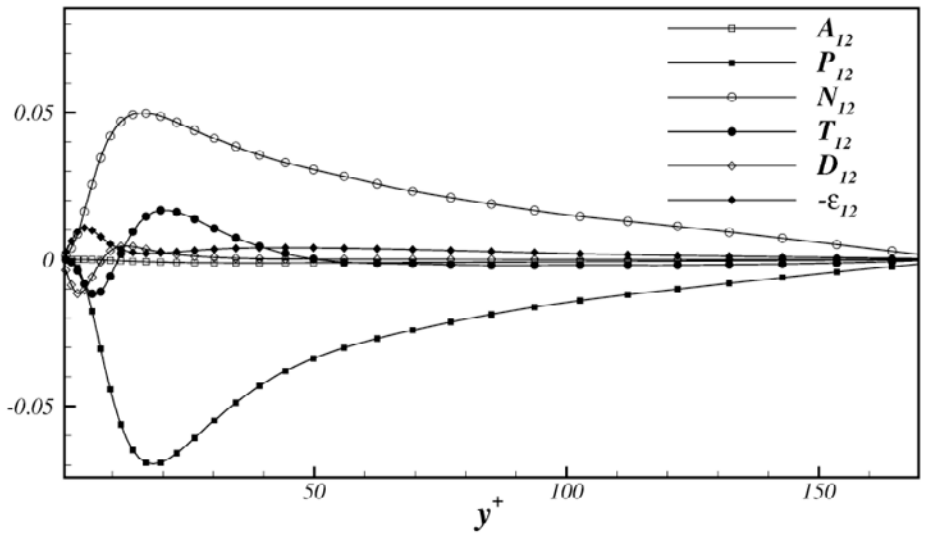

(a)

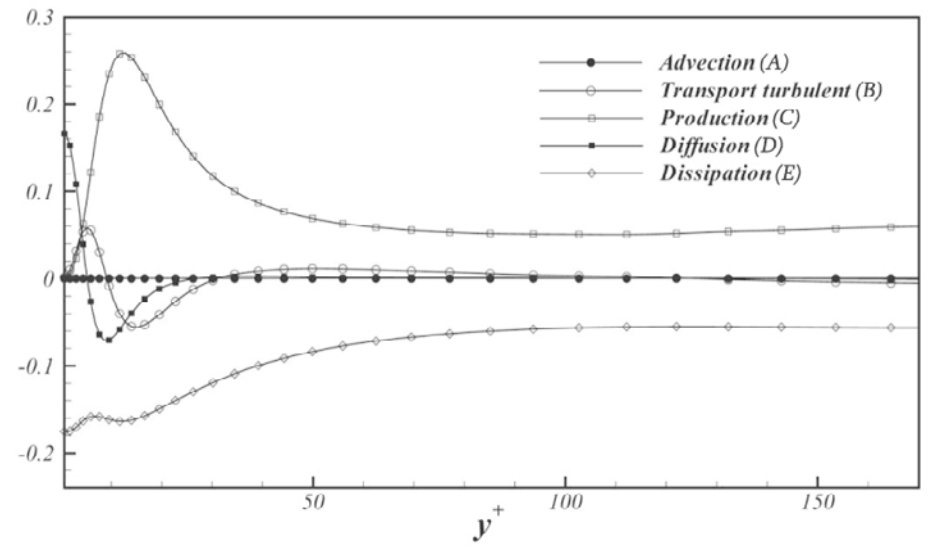

(b)

Fig. 2. Distribution of the terms appearing in the Reynolds shear stress transport equation (a) and the temperature fluctuations (b) in the standard turbulent channel flow.

The turbulent drag is due to the presence of the QSV whose destruction is necessary for drag reduction, in which case their beneficent effect on the mixing is also suppressed. The fact that the coherent structures are directly linked to the turbulent transfer activity may be more clearly seen in Fig. 3(b) that shows the fluctuating temperature field in the presence of λ_2 structures. High positive and negative fluctuating T'^+ zones are found respectively at the sweep and ejection sides of the QSV. This is expected because of the high correlation existing between temperature and streamwise velocity fluctuations. Forcing locally the wall turbulence in someway may eventually lead to the active control of both the drag and Nusselt numbers, yet the existing active control strategies are presumably not suitable to achieve this goal.

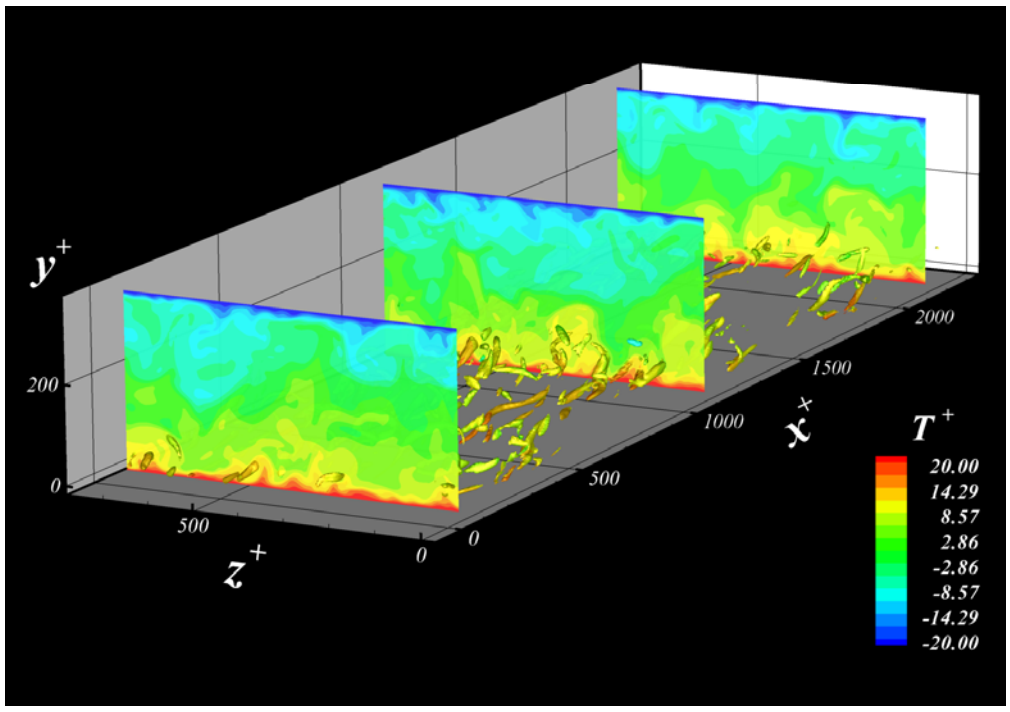

(a)

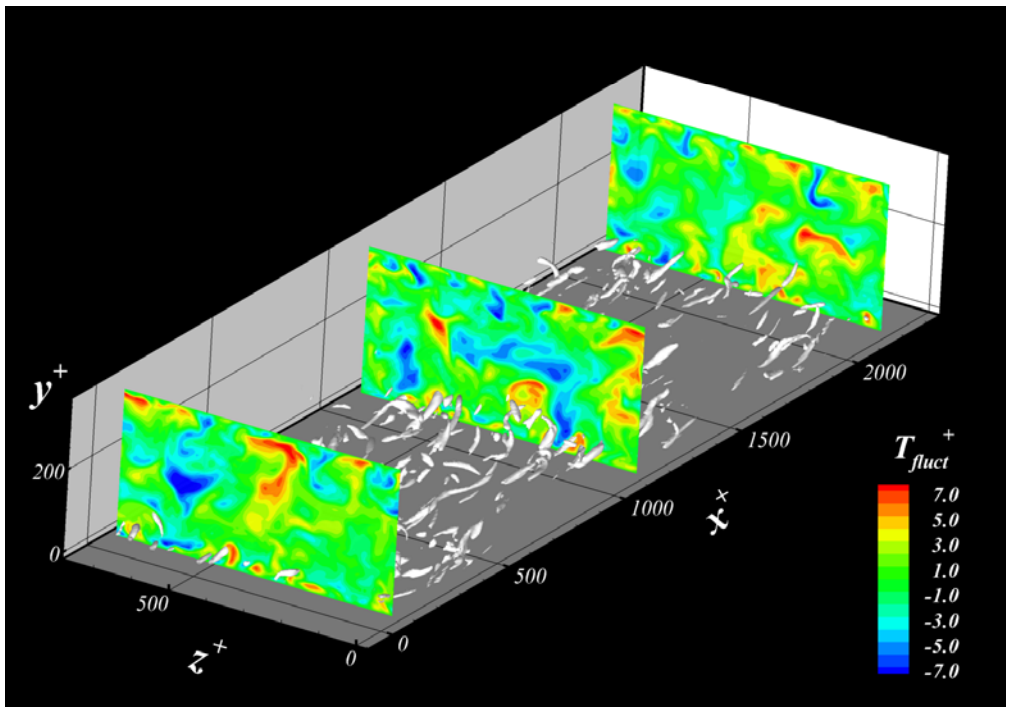

(b)

Fig. 3. Coherent structures and associated instantaneous temperature (a) and temperature fluctuations (b) in the standard turbulent channel flow.

4. Results

The results obtained under the effect of the localized blowing (Fig. 1) with small severity will now be discussed. The spatial evolution of the wall shear $\overline{\tau}^+$ and wall heat flux $-\overline{q}^+$ in the streamwise direction over and downstream the slot is shown in Fig. 4(a). Both quantities are scaled by the inner variables of the standard turbulent wall layer to sort out the direct effect of local blowing. It is seen that the shear is approximately equal to the heat flux, i.e. $\overline{\tau}^+ \approx -\overline{q}^+$ immediately downstream the slot, indicating that the Reynolds analogy holds acceptably well. This is however not entirely true over the slot, where the heat flux reaches $-\overline{q}^+ = 0.4$ while $\overline{\tau}^+ \approx 0.7$ pointing at some confined disequilibrium effects. The fluctuations of the wall flux are indeed more intermittent compared to τ' as it is seen in Fig. 5 that shows the flatness $F(q') = \dfrac{\overline{q'^4}}{\left(\overline{q'^2}\right)^2}$ of the q' and τ' fluctuations. The wall shear and flux turbulent intensities however collapse quite well both over and downstream the slot (Fig. 4(b)). Note the large decrease of the turbulent activity at the leading edge of the slot where both the shear and the shear stress intensity, together with $-\overline{q}^+$ and q^+_{RMS} decrease by 50%, showing clearly a tendency of the flow to relaminarize over the slot under small severity parameter that avoids flow separation.

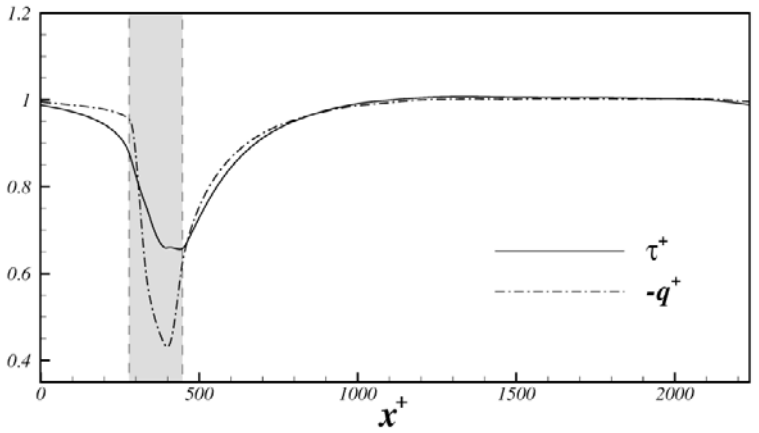

Fig. 4. Streamwise evolution of the wall shear stress and heat flux (a) and turbulent shear and flux intensities (b) under steady blowing.

The fluctuating streamwise velocity decreases also downstream the slot and typically in the buffer layer. Figure 6(a) shows the contours of the relative $u'^{+}_{RMS(rel)}$ defined as $u'^{+}_{RMS(rel)} = u'^{+}_{RMS} - u'^{+}_{RMS(SF)}$ where (SF) stands for the standard unmanipulated flow. A similar representation will be used hereafter for other quantities Q with $Q_{(rel)} = Q - Q_{(SF)}$. It is seen that the streamwise turbulent intensity decreases quite significantly in the low buffer layer at $y^{+} < 10$ followed by only a slight increase at $y^{+} \approx 20$ contrarily to Park and Choi (1999) who noticed an increase of turbulence activity. It has to be emphasized that the severity parameter used by these authors is twice larger than ours, and the flow is consequently separated downstream the slot, while we paid special attention to avoid the separation in this investigation. The same behavior holds also for the Reynolds shear stress significantly lower over the slot compared to the standard boundary layer (Fig. 6(b)).

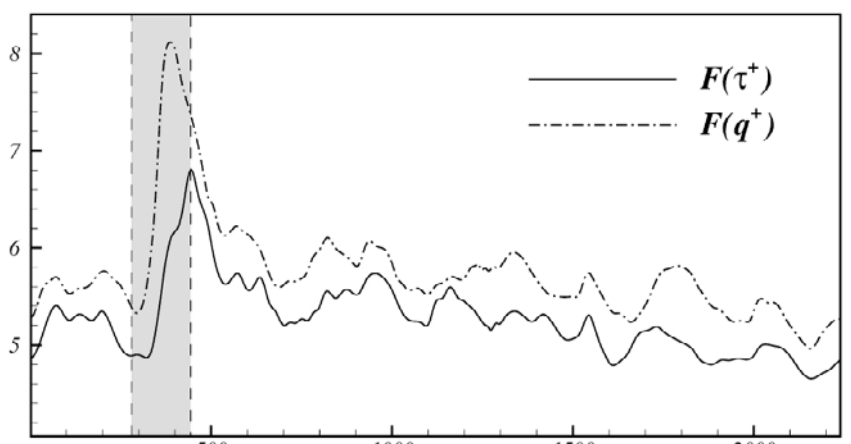

Fig. 5. Flatness of the fluctuating wall shear and wall flux. Note the high intermittency of the instantaneous temperature gradient within the slot.

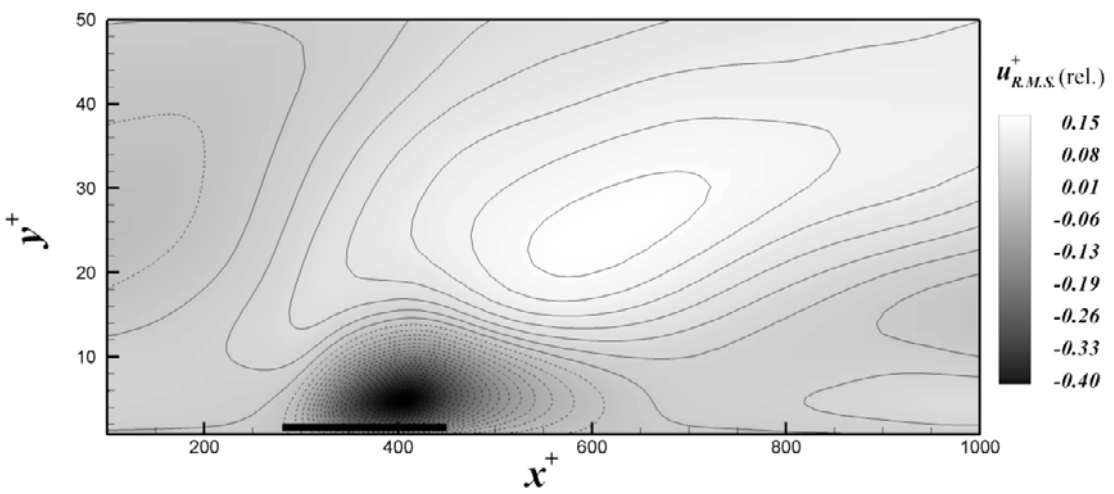

(a)

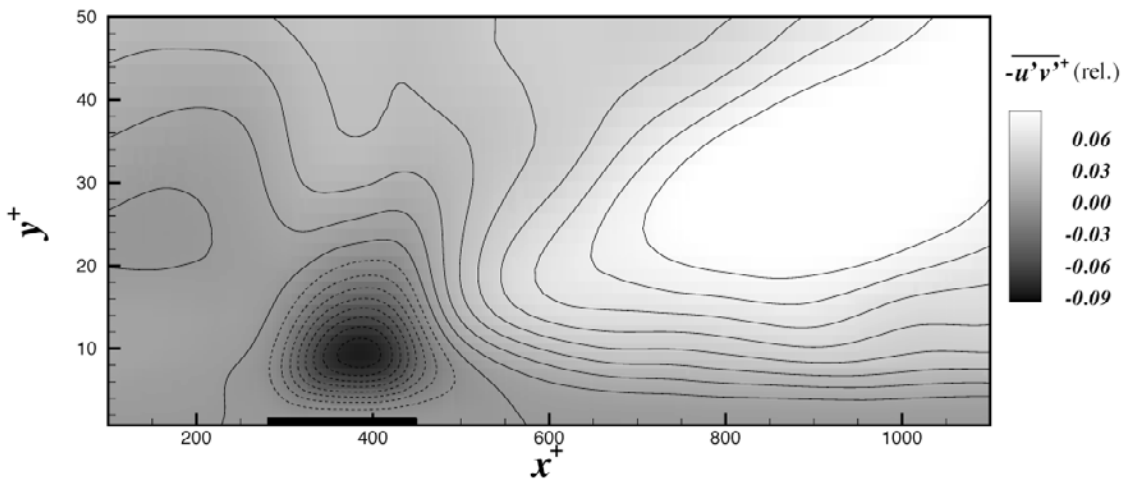

(b)

Fig. 6. Longitudinal relative turbulent intensity (a) and Reynolds shear stress (b).

All the terms appearing in the transport equation of the Reynolds shear stress $-\langle u'v' \rangle = -\langle u'_1 u'_2 \rangle$ have been carefully analyzed. The most pronounced effects of the local blowing have been found on the production P_{12} and pressure redistribution N_{12} terms (Eq. 1). The production under the local blowing is $P_{12} = -\langle v'v' \rangle \frac{\partial \langle u \rangle}{\partial y} - \langle u'u' \rangle \frac{\partial \langle v \rangle}{\partial x}$, while in the channel flow the second term is strictly zero. The effect of the induced wall normal velocity gradient $\frac{\partial \langle v \rangle}{\partial x}$ is confined near the trailing and leading edges of the slot as expected. Figure 7 shows the distribution of $P_{12(rel)} = P_{12} - P_{12(SF)}$. It is seen that the production increases near the leading edge of the slot and its effect is extended both downstream and in the log-layer. The maximum production excess takes place slightly upstream of the leading edge at $y^+ = 15$ where the production reaches its maximum in the standard flow. Near the trailing edge, in return the production decreases by nearly 50 % at $y^+ \approx 12$. The behavior of the production over the slot is rather complex and difficult to explain. At the trailing edge the Reynolds shear stress producing eddies are suddenly pushed away from the wall and both the shear and $\langle v'v' \rangle$ decrease suddenly. The information is felt in the pressure distribution terms N_{12} rapidly that increases in this zone as shown in Fig. 8. The pressure-velocity terms redistribute energy to wall normal velocity component that consequently increase immediately downstream this zone causing the subsequent increase in the production. That causes the strong decrease of N_{12} and the situation is just inversed. Immediately near the leading edge and downstream the slot the decrease in pressure-velocity redistribution relaxes rapidly the production to decrease. At the final the sum $P_{12(rel)} + N_{12(rel)}$ becomes negative, causing the decrease of the Reynolds shear stress shown in Fig. 6(b). Generally speaking the decrease in N_{12} is stronger than the increase in the production. The consequent decrease in $-\langle u'v' \rangle$ is essentially due to the delay in time and space between production and pressure-velocity correlations. Note the high complexity in the inter-component transfer process due to the strong local disequilibrium induced by sudden change of the boundary conditions. It is impossible to draw conclusions in such flows from the analysis of limited flow quantities, and the whole process has to be carefully taken into account.

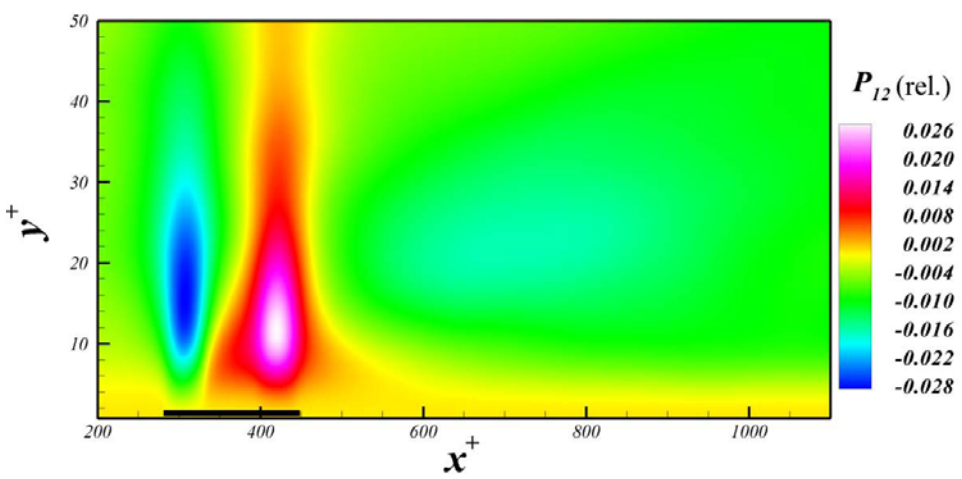

Fig. 7. Relative production near the blowing slot shown by a thick line on the figure.

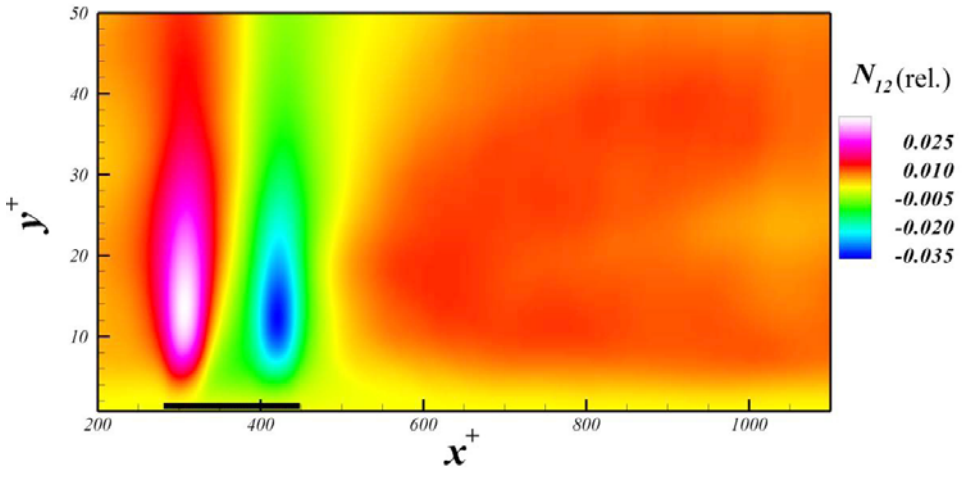

Fig. 8. Relative pressure redistribution near the blowing slot.

Figure 9 shows the distribution of the modified temperature θ non-dimensionalized with respect to local wall transfer variables i.e. local u_τ and q at a given streamwise position x^+ downstream the slot. The global observation is that the temperature increases over and downstream the slot because the local blowing pushes away the hot layers towards the channel centerline. The θ^+ collapses with the profile of the standard flow at $x^+ = 200$ and the temperature relaxation takes place earlier that the streamwise velocity u^+ which relaxes at $x^+ = 500$ (not shown here), indicating that the local wall similarity between the velocity and temperature does not exactly hold due to the imposed disequilibrium. The temperature fluctuations θ'^+_{RMS} increase considerably over the slot as it is seen in Fig. 10, and the relaxation is not entirely established at $x^+ = 200$ particularly in the buffer layer.

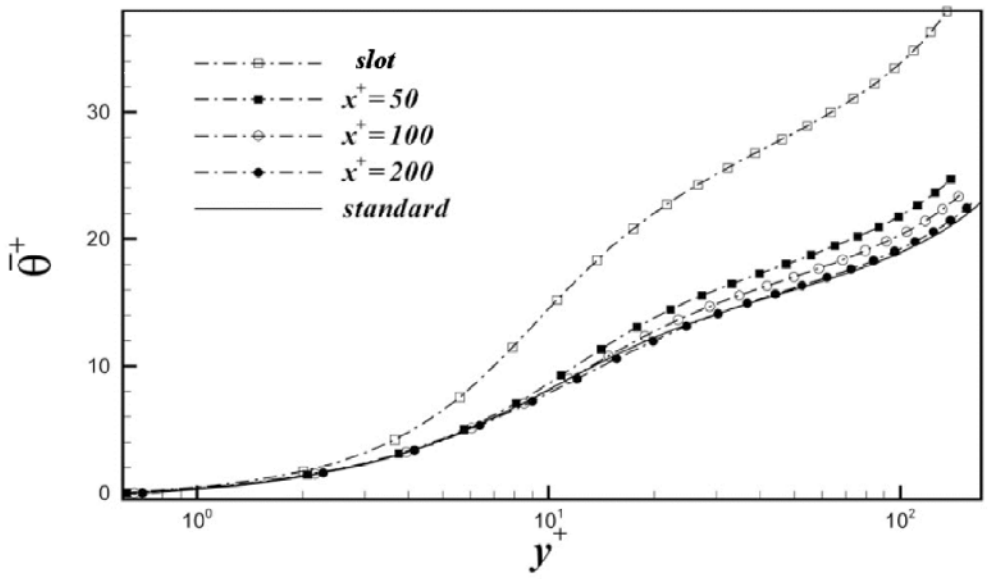

Fig. 9. Modified temperature in local variables over and downstream the slot.

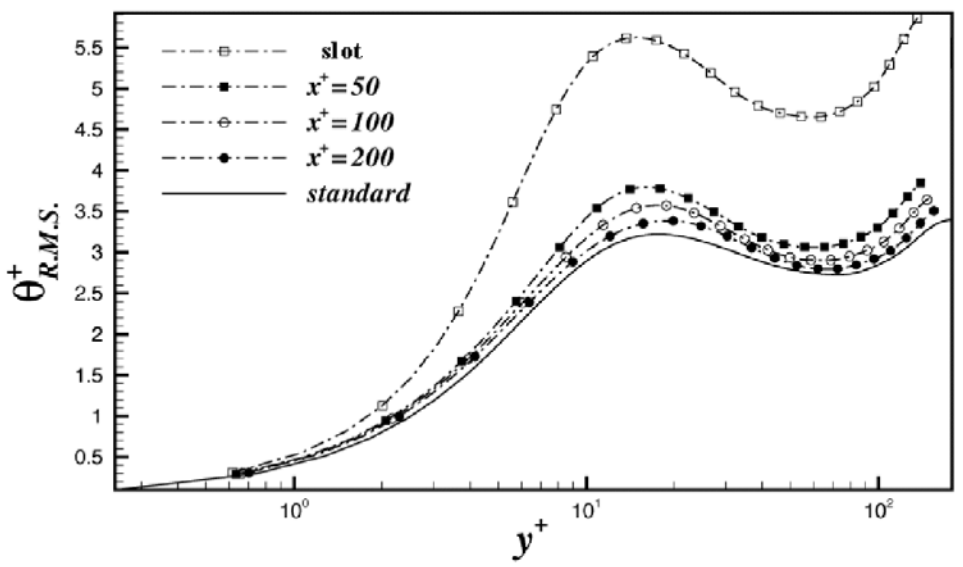

Fig. 10. RMS of modified temperature fluctuations in local variables over and downstream the slot.

The advection $A=-\frac{1}{2}\overline{u}\frac{\partial\overline{T'^2}}{\partial x}-\frac{1}{2}\overline{v}\frac{\partial\overline{T'^2}}{\partial y}$ governing the transport process of the temperature fluctuations (Eq. 2) is zero in standard turbulent channel flow. It plays an important role in the transfer process over the slot. Figure 11 shows its distribution ($A_{(rel)}=A$). The advection is significantly negative over the slot, and becomes slightly positive downstream in the internal layer. All the terms appearing in Eq. 2 are roughly equally affected by the local blowing contrarily to the Reynolds shear stress transport equation wherein the production and the pressure redistribution terms are mainly modified as we have just discussed. The production $C=-\overline{u'T'}\frac{\partial\overline{T}}{\partial x}-\overline{v'T'}\frac{\partial\overline{T}}{\partial y}$ for instance is increased by nearly 40% near the trailing edge at $y^+=15$ (Fig. 12). Note that this is

opposite to the production of the shear stress P_{12} (Fig. 7) that decreases in this zone. The zone wherein the production is increased extends to 20 to 40 wall units in the direction normal to the wall and approximately 250 wall units in the longitudinal direction. This is due to the displacement of the quasi-streamwise structures from the buffer layer to the low log-layer. Near the leading edge, in return, and in the low buffer layer, the production C decreases significantly, once more contrarily to the behavior of P_{12}.

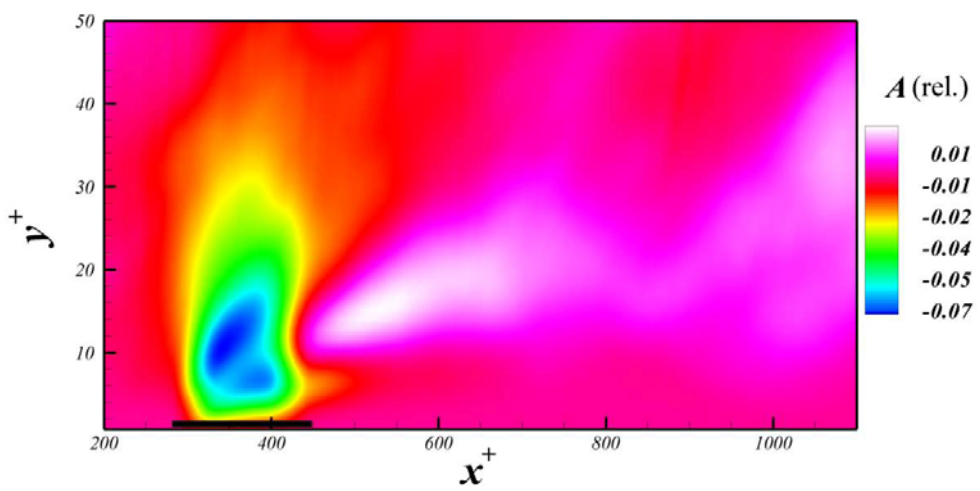

Fig. 11. Advection term appearing in the temperature fluctuations transport equation.

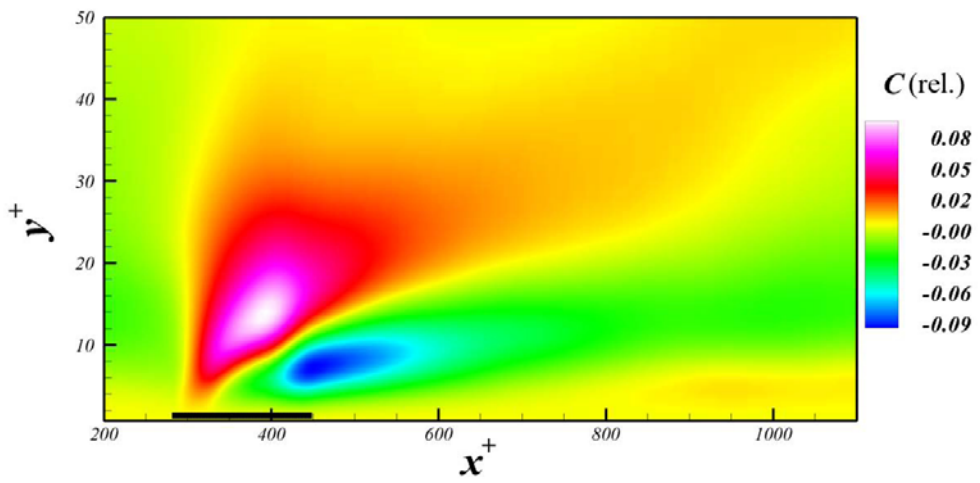

Fig. 12. Relative production of the temperature fluctuations transport equation.

The relative dissipation, $E_{(rel)} = E - E_{(SF)}$, shown in Fig. 13, with:

$$E = -\frac{1}{PrRe}\left\{\overline{\left(\frac{\partial T'}{\partial x}\right)^2} + \overline{\left(\frac{\partial T'}{\partial y}\right)^2} + \overline{\left(\frac{\partial T'}{\partial z}\right)^2}\right\}$$

is strongly positive over the slot, indicating that it decreases in absolute value in this zone ($E < 0$). It is typically $E = -0.04$ at the wall, which is quite low compared to $E = -0.16$ of the standard flow (Fig. 2(b)).

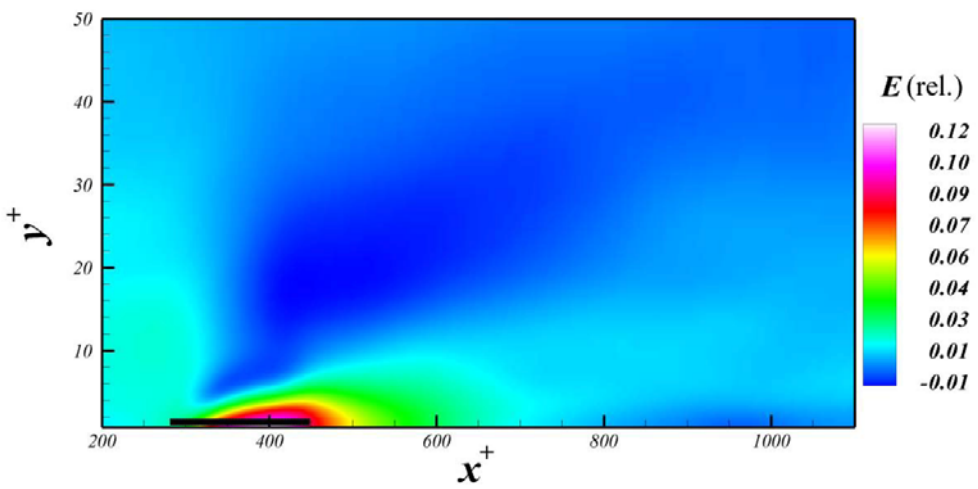

Fig. 13. Relative dissipation of the temperature fluctuations transport equation.

5. Conclusion

The effect of localized blowing through a slot on the wall turbulence structure and transfer process has been analyzed by direct numerical simulations. The blowing severity parameter is mild and there is no induced flow separation. We have shown that both the wall shear stress and the wall flux decrease downstream the slot, and the Reynolds analogy is valid except over the slot where the wall flux decrease more than the shear stress. The flow is in strong non-equilibrium despite the mild blowing severity. The production and the pressure redistribution play an essential role in the response of the turbulence in the buffer layer. The ensemble of temperature fluctuations transport terms is structurally modified with respect to the standard unmanipulated wall turbulence. Besides its own importance, the local blowing constitutes a way to analyze the response of wall turbulence to a sudden modification of boundary conditions at the wall, and its subsequent relaxation.

References

Andersen, P.-S., Kays, W.-M. and Moffat, R.-J., Experimental results for the transpired turbulent boundary layer in an adverse pressure gradient, J. Fluid Mech., 69 (1975), 353-375.

Chakraborty, P., Balachandar, S. and Adrian, R.-J., Kinematics of local vortex identification criteria, J. of Visualization, 10-2, (2007), 137-140.

Jeong, J. and Hussain, F., On the identification of a vortex, J. Fluid Mech., 285 (1995), 69-94.

Kawamura, H., Ohsaka, K., Abe, H. and Yamamoto, K., DNS of turbulent heat transfer in channel flow with low to medium-high Prandtl number fluid, Int. J. Heat and Fluid Flow, 19 (1998), 482-491.

Lyons, S., Hanratty, T. and McLaughin, J., Direct numerical simulation of passive heat transfer in a turbulent channel flow, Int. J. Heat and Mass Transfer, 34-4/5 (1991), 1149-1161.

Mansour, N., Kim, J. and Moin, P., Reynolds shear stress and dissipation rate budgets in a turbulent channel flow, J. Fluid Mech., 122 (1988), 15-44.

Park, J. and Choi, H., Effect s of uniform blowing or suction from a spanwise slot on a turbulent boundary layer flow, Phys.

Fluids., 11-10 (1999), 3095-3105.
Sano, M. and Hirayama, N., Turbulent boundary layers with injection and suction through a slit, Bulletin of JSME, 28 (1985), 807-814.
Sokolov, M. and Antonia, R.-A., Response of a turbulent boundary layer to intensive suction through a porous strip, Ninth Symp. on Turbulent Shear Flows (Kyoto), (1993), 5-3-1 to 5-3-6.
Tardu, S., Near wall turbulence control by time space periodical blowing and suction. Effect of local time periodical blowing, Exp. Thermal and Fluid Science, 16/1-2, (1998), 41-54.

Author Profile

Sedat Tardu: He received his B. Sc and M. Sc. (Mechanical Engineering) conjointly from Technical University of Istanbul, and the Polytechnic Institute of Grenoble in 1982 and 1984, his Ph.D and Habilitation in respectively 1988 and 1994 from the University of Grenoble wherein he is currently an associate professor. He has been an invited researcher and a professor at Ecole Polytechnique Fédérale de Lausanne and at Imperial College, London. His research interests include, unsteady turbulent boundary layers with and without adverse pressure gradient, wall turbulence, active and passive control, microfluidics, and micromixing through experimental and computational strategies. He is an author of about 80 journal and book papers and more than 100 communications in proceedings.

Olivier Doche: He received his B.Sc and M. Sc (Mechanics) from the University of Grenoble in respectively 2002 and 2003 and his PhD from the same University in 2006. After postdoctoral research at CEA (French Nuclear Research Center) wherein he worked on nanofluids, he joined recently AREVA as a senior research engineer. His main research interests are computational fluid dynamics, direct numerical simulations active and passive control of turbulent drag.